HHS Public Access

Author manuscript

Anal Chem. Author manuscript; available in PMC 2016 August 04.

Published in final edited form as:

Anal Chem. 2015 August 4; 87(15): 7887–7893. doi:10.1021/acs.analchem.5b01669.

Functionalized Polymer Microgel Particles Enable Customizable Production of Label-Free Sensor Arrays

Mark A. Lifson[†], **Jared A. Carter**[‡], and **Benjamin L. Miller**[†,§,*]

[†]Department of Biomedical Engineering, University of Rochester, Rochester, New York 14627, United States

[§]Department of Dermatology, University of Rochester, Rochester, New York 14627, United States

[‡]Adarza BioSystems, Inc. West Henrietta, New York 14586, United States

Abstract

Probe molecule immobilization onto surfaces is a critical step in the production of many analytical devices, including labeled and label-free microarrays. New methods to increase the density and uniformity of probe deposition have the potential to significantly enhance the ultimate limits of detection and reproducibility. Hydrogel-based materials have been employed in the past to provide a 3D protein-friendly surface for deposition of antibodies and nucleic acids. However, these methods are susceptible to variation during polymerization of the hydrogel scaffold, and provide limited opportunities for tuning deposition parameters on an antibody-by-antibody basis. In this work, a versatile hydrogel nanoparticle deposition method was developed for the production of label-free microarrays, and tested in the context of antibody-antigen binding. Poly (N-isopropylacrylamide) nanoparticles (PNIPAM) were conjugated to antibodies using an avidin/biotin system and deposited onto surfaces using a noncontact printing system. After drying, these gel spots formed uniform and thin layers < 10 nm in height. The conjugates were characterized with dynamic light scattering, scanning electron microscopy, and atomic force microscopy. We tested this format in the context of tumor necrosis factor-alpha (TNF-α) detection via Arrayed Imaging Reflectometry (AIR), a label-free protein microarray method. This method of probe molecule deposition should be generally useful in the production of microarrays for label-free detection.

There is a significant interest in developing microarray technologies to monitor the presence, amounts, and activities of many classes of biomolecules. In addition to obvious advantages in throughput, microarray methods for protein detection have been posited to yield remarkable improvements in accuracy and sensitivity because of a reduction in the interaction area of the target and receptor.[1–3] As such, there has been a major effort to

[*]**Corresponding Author**benjamin_miller@urmc.rochester.edu.

ASSOCIATED CONTENT

Supporting Information Available: This material is available free of charge via the Internet at http://pubs.acs.org/.

Notes

J. A. C. is an employee of Adarza BioSystems, Inc., which is involved in commercializing the AIR technology. B. L. M. is a board member and advisor of Adarza BioSystems, Inc.

immobilize hundreds to thousands of probe molecules on a single device to globally analyze the binding of targets in a high-throughput manner.[4–7]

A microarray consists of a rigid support, on which biomolecules are immobilized in an addressable way, so that each printed region (spot) is specific for one target in a sample of interest. In this format, a wide variety of proteins, nucleic acids, or small molecules can be targeted by immobilizing different probe biomolecules including proteins, peptides, antibodies, sugars, enzymes, or aptamers with the requisite specificities.[5,7–9] Binding of the target is most often detected by measuring fluorescence intensity changes from labeled tags either on the target itself (direct mode), or on a 2° antibody (sandwich). Alternatively, new microarray formats have been developed that directly measure target concentrations via changes in the optical properties of the sensor itself as a function of bound target.[10–13] These label-free technologies can have high sensitivities, but often have more stringent requirements for regular and uniform deposition of capture molecules, as compared to fluorescent methods, which are insensitive to localized variability in the z direction.[14,15] Regardless of the type of assay, the surface functionalization and immobilization procedures must be carefully considered since these directly affect the probe density and orientation on the substrate, which in turn affects the amount of target bound.[16–18] It has been observed that directly immobilizing biomolecules onto planar surfaces results in significant unfolding/denaturing of proteins, translating to a loss of ligand binding activity, adversely affecting the assay's ultimate performance.[19–21] Thus, increasing the density, uniformity and integrity of probe molecules on planar surfaces is an important subject of research.

One approach to increase antibody density onto surfaces is to incorporate them within a 3D matrix as opposed to a 2D surface. The materials of choice for this purpose are hydrogels, due to their high surface areas, biocompatibility, and straightforward bioconjugation to biomolecules. By providing a more "solution-like" environment for attached probe molecules, hydrogels may also reduce surface-induced denaturation.[22] Hydrogels are typically applied to substrates in one of two ways: either the network is coated prior to biomolecule immobilization, or, hydrogel precursors are spotted with biomolecules and polymerized in situ.[23–30] However, many label-free microarray technologies are incompatible with these processes, since they produce thick hydrogel layers with significant variations in coating thickness and porosity.[31–33] This is part of the reason why ultra-sensitive methods continue to use 2D immobilization strategies for capture molecules.[34–38] Both strategies also limit the degree to which probe molecule deposition may be optimized on a probe-by-probe basis: the pre-existing hydrogel matrix (since the underlying substrate is the same for all probes), and the post-spotting polymerization method (as this is constrained by the requirements of the polymerization reaction).

In this paper, we describe a new technique to deposit thin and reproducible hydrogel layers onto rigid surfaces for optical label-free microarrays. We find that Poly (N-Isopropylacrylamide) (PNIPAM) nanoparticles conjugated with capture molecules self-assemble into highly reproducible and uniform monolayers upon drying after microprinting on a substrate. PNIPAM hydrogel nanoparticles were co-polymerized with allylamine (AA) so that after synthesis, free amines could be covalently linked with biotin using an amine-reactive functional group (N-hydroxysuccinimide). Upon addition of avidin with the

particles, biotinylated probe molecules were linked to the particles in a single conjugation step in a “sandwich” format. This method is highly modular and could potentially be used to create a library of particle-probe entities.

We used a highly sensitive protein microarraying technology, Arrayed Imaging Reflectometry (AIR), to evaluate the performance of hydrogel nanoparticle microarrays. AIR operates by measuring the light intensity of an angled beam reflected off of a flat substrate, which is composed of a protein-reactive film on a thermally grown silicon oxide layer. If the angle, wavelength, and polarization of the incident light beam is fixed, a near-zero reflectance condition can be obtained by adjusting the thickness of the thermally grown oxide. The relationship between the intensity of reflection and thickness has been well characterized both experimentally and theoretically by our group, and has enabled quantitative evaluation of biological systems including affinity constants for antibodies and targets.[39–44] Though this work discusses the specifics of applying a hydrogel network onto AIR substrates, the methods, materials, and techniques could be easily applied to other label-free sensor technologies that require thin and uniform coatings, and may also have utility for labeled microarray technologies.

Experimental Section

Materials

Poly (N-isopropylacrylamide), bisacrylamide, sodium dodecyl sulfate, allylamine, zero-link or long-chain biotin and O-phthalaldehyde were purchased from Sigma Aldrich. Avidin was purchased from Rockland Immunochemicals. Anti-human tumor necrosis factor alpha IgG (a-TNF-α) and TNF-α were purchased from Biolegend. Silicon substrates with thermally grown oxide both with and without amine reactive surfaces were provided by Adarza BioSystems.

PNIPAM-co-allylamine synthesis

Poly(N-isopropylacrylamide) co-allylamine microgels were prepared via a free radical precipitation polymerization method modified from the literature.[45–48] Briefly, (N-isopropylacrylamide) (NIPAM) (130 mM), allylamine (13 mM), bis-acrylamide (BIS) (1.7 mM), and sodium dodecyl sulfate (SDS) (1.1 mM) were dissolved in 50 mL of deionized, glass-distilled H2O (ddH2O) inside a 500 mL 3-neck flask equipped with a nitrogen line, overhead stirrer, and gas outlet, then stirred thoroughly. Next, the solution was bubbled with nitrogen for 45 min to remove dissolved oxygen. The mixture was then heated to 60 °C, and ammonium persulfate (2.5 mM) was added into the flask to start the reaction. The reaction proceeded for 5 hours, and produced a cloudy suspension indicating the formation of particles. The flask was then removed from heat and opened to ambient atmosphere while maintaining a constant stir rate for 15 min. Lastly, 5 mL of suspended particles were dialyzed for a minimum of 24 hours with 3 exchanges against ddH2O. PNIPAM particles without amine reactivity were synthesized analogously, absent the presence of allylamine. Since it was difficult to accurately determine the concentration of particles in terms of particle number, particles were tracked by their dilution from stocks (e.g. a 1/10 dilution of particles implies stock particles were diluted 10-fold, whereas 1/100 would be 100-fold).

Biotinylation of PNIPAM-co-allylamine

To conjugate biotin to PNIPAM-co-allylamine (PNIPAM-co-AA) particles, 2 mg of long-chain NHS-biotin was dissolved in 100 μL of DMF, and 20 μL of this solution was added to 1 mL of 1/10 PNIPAM-co-AA particles in modified phosphate buffered saline buffer (mPBS) (10 mM NaH2PO4, 10 mM Na2HPO4, 150 mM NaCl at pH 7.2). The particles were agitated using a tube rotator at room temperature for 2 hours and dialyzed extensively against de-ionized glass-distilled water (ddH2O).

Detecting amine content using o-phthalaldehyde

Reaction with o-phthalaldehyde was used to measure the amine functional groups present on PNIPAM particles. O-phthalaldehyde (15 mg), β-mercaptoethanol (10 μL), and ethanol (300 μL) were dissolved in 10 mL of 50 mM sodium carbonate buffer (pH=10.5). The reagent was always prepared at most 2 hours prior to use to ensure freshness. Several allylamine concentrations (50, 5, 0.05, 0.005, and 0.0005 mM) were used to establish a calibration curve; 100 μL of allylamine was prepared at each concentration and mixed with 100 μL of reagent in one well of a 24-well plate. In the same plate, 100 μL of different dilutions (1/10, 1/100, 1/1000) of PNIPAM, PNIPAM-co-AA, and PNIPAM-co-AA-biotin with unknown amine content were mixed with 100 μL of working reagent. Samples were equilibrated for 90 seconds, and then absorbance was measured spectrophotometrically at 410 nm.

Avidin conjugation

A 1/10 dilution of PNIPAM-co-AA-biotin particles in mPBS (pH = 7.2) was mixed with an equal volume of 20 mg/mL avidin (final concentration 10 mg/mL) and incubated for 6 hours at 4 °C while rotating on a tube rotator. The particles were then dialyzed extensively against ddH2O using a membrane with molecular weight cutoff of 150 kDa.

Antibody conjugation

Biotinylated and avidinylated PNIPAM-co-allylamine diluted 1/35 was pre-mixed with biotinylated antibody at 200 μg/mL (final concentration 100 μg/mL) and allowed to stand for at least 6 hours at 4 °C in a 384-well plate. This solution was used directly for printing.

Size determination by Dynamic Light Scattering

Particle size measurements were performed using dynamic light scattering with a Malvern ZS90 Zetasizer (Malvern Instruments; Malvern, United Kingdom). Particles were diluted 1/1000 in deionized distilled water before measuring z-average diameter and polydispersity index (PDI). The number of runs was automated by the Malvern software, but was ensured to be always greater than n=3.

Microarray spot deposition

All solutions to be printed were pipetted individually into a 384-well plate at 20 μL volumes. PNIPAM-co-AA and PNIPAM-co-AA-biotin were diluted in water. PNIPAM-avidin was diluted in 150 mM mPBS. An S3 Sciflexarrayer (Scienion A.G.; Berlin, Germany) with a PDC90 capillary was used to print probes inside a humidity chamber at 60-80% RH. Droplets were between 200-300 pL in volume as measured by the instrument. After

deposition, spots were analyzed with an overhead camera to ensure their uniformity and to monitor their drying behavior. Once spots had dried, substrates were removed from the humidity chamber and used for experiments.

Dry spot analysis

Particles were visualized with an Auriga CrossBeam SEM-FIB scanning electron microscope (Zeiss; Jena, Germany) at 0.5 kV. The surface topography of spotted microgels was analyzed with a Solver Next atomic force microscope (NT-MDT; Moscow, Russia). Interparticle distance and particle size calculations using the AFM image were performed using ImageJ (v. 1.48k) and custom MATLAB software routines.

Imaging with Arrayed Imaging Reflectometry

All microarrays were imaged on a prototype AIR imaging system (Adarza BioSystems; NY, USA). Images were acquired for each substrate using custom in-house instrument control software at 10, 50, 100, 250, 500, and 750 millisecond exposure times. Spot intensities were measured using ImageJ (v. 1.48k) and converted to thicknesses using a best-fit line to a reflectance model.[49] Average measurements were composed of at least three spots, with errors represented by standard deviations of these measurements.

Target detection on immobilized PNIPAM-co-AA nanoparticle microspots

PNIPAM-co-AA and PNIPAM-co-AA-biotin were diluted in water and spotted onto AIR substrates (thermal oxide 135.5 nm) using a piezoelectric microarrayer. After printing the particles, a second layer of spots was placed over the first (overspots) of biotinylated anti-TNF-α antibodies at a concentration of 10 nM in mPBS. After spots had dried, substrates were immediately placed into wells inside of a 24-well plate containing 1% BSA in 50 mM HEPES buffered saline (20 mM HEPES, 150 mM NaCl, pH 7.2) for 30 minutes to block the background from non-specific adsorption. Substrates were then transferred to wells containing 10 nM TNF-α in mPBS buffer and incubated for 1 hour with shaking, followed by mPBS incubation for 30 minutes, and water for 5 minutes before drying and imaging. Substrates were withdrawn after each stage to monitor the thickness change by AIR.

Target detection using antibody conjugated PNIPAM-avidin nanoparticle microspots

PNIPAM-avidin and PNIPAM-co-AA-biotin diluted 1/35 in mPBS, were mixed with biotinylated anti-TNF-α antibodies (200 μg/mL in mPBS), anti-TNF-α antibodies (200 μg/mL in mPBS), or 1% BSA in mPBS. Particles were spotted onto AIR substrates (thermal oxide 135.5 nm) using a piezomicroarrayer as described above. After spots had dried, substrates were immediately placed into wells inside of a 24-well plate containing 1% BSA in 50 mM HEPES buffered saline (20 mM HEPES, 150 mM NaCl, pH 7.2) for 30 minutes to block the background from non-specific adsorption of target. Substrates were then incubated with TNF-α (for selectivity study, concentration was 10 nM, for limit of detection concentration was 1 pg/mL – 100 ng/mL in 10-fold increments) overnight at room temperature in a humidity chamber (~80% R.H.) with shaking. Substrates were then washed in mPBS for 30 minutes followed by a 5 minute deionized double distilled water wash before drying and imaging.

Results and Discussion

The central goal of this work was to develop a uniform hydrogel coating that would be compatible with label-free microarrays. To accomplish this, hydrogel nanoparticles capable of binding biotinylated probe molecules were synthesized by converting incorporated amine functionalities to biotin, and then linking particles with avidin.

Particle synthesis and evaluation

Hydrogel nanoparticles with amine functionality were synthesized in a homogenous radical precipitation polymerization combining (N-isopropylacrylamide) (NIPAM), allylamine (AA), and bis-acrylamide (bisA) monomers to form Poly (N-isopropylacrylamide) and allylamine co-polymerized particles (PNIPAM-co-AA). Particle-bound free amines were reacted with NHS-biotin in a covalent, one step process (PNIPAM-co-AA-biotin). As a control, particles containing no free amines were synthesized from only NIPAM and bisA. To confirm and quantify successful biotinylation of PNIPAM-co-AA particles, an o-phthalaldehyde (OPA) assay was used to quantify free amines for different dilutions of PNIPAM-co-AA, PNIPAM-co-AA-biotin, and PNIPAM control particles (Figure 1).[50]

The number of amines present on PNIPAM-co-allylamine (PNIPAM-co-AA) particles was evaluated to be 163 ± 4.12 μmol/L for particles diluted 1/10, and 22.4 ± 0.01 μmol/L for particles diluted 1/100 (black bar). As expected, the amine content decreased by approximately one order of magnitude. At a higher dilution of 1/1000, the measured amine concentration was not significantly different from that found in the PNIPAM control (white hatched bar), due to reaching the noise floor of the assay at ~5.5 μmol/L. Biotinylated PNIPAM-co-allylamine particles (gray vertical striped bar) had approximately 15 times less amine content compared to PNIPAM-co-AA particles (10.7 ± 0.21 μmol/L) and were found to be only slightly higher than the PNIPAM control (8.6 ± 0.01 μmol/L) suggesting that almost all available amines were biotinylated. More concentrated solutions of particles were not evaluated due to the large volume of particle samples required for the OPA assay.

Next, avidin was allowed to bind to PNIPAM-co-AA-biotin forming PNIPAM-avidin particles. The average diameters were evaluated by dynamic light scattering at each consecutive step (Figure 2). PNIPAM-co-AA, PNIPAM-co-AA-biotin, and PNIPAM-avidin particles had z-average diameters of 221±68.3 nm, 237.0±53.5 nm, and 248.5±87.2 nm respectively. The polydispersity indices, which are related to the standard deviations,[51] were 0.095, 0.051, 0.123 respectively indicating that the particles were monodisperse after each step.

Conjugation of biotin and avidin appeared to have no effect on particle size, suggesting that the morphology and size of the particles was constant, with no evidence of either aggregation or precipitation within the solution. This was expected, since PNIPAM nanoparticles are a mesh-like material where significant space within the mesh is taken up by the solvent (water or buffer); conjugation of a protein likely displaced solvent instead of adding thickness.

Evaluating particle compatibility with piezo-microspotting methods

Hydrogel nanoparticles were evaluated for their potential application as a substrate for a label-free protein microarray. First, it was essential to determine if particles were compatible with spotting via a piezoelectric microarrayer. Two different array fabrication modes were envisioned: (1) spotting of biotin-conjugated particles followed by overspotting with avidin and antibody,and (2) spotting of biotinylated particles premixed with both avidin and biotinylated antibody. Both of these methods were examined separately. In initial experiments, PNIPAM-co-AA-biotin particles were diluted in ddH_2O at various concentrations, spotted with ~300 pL volumes onto a silicon substrate, and imaged using AIR (Figure 3). AIR images of arrays showed that although particles were successfully deposited, particle concentration-dependent differences in spot morphology were observed. At the highest concentration (1/40, lowest dilution) spots with bright rings and dark centers were present due to accumulation of particles at the outer edges after drying. Smaller differences became apparent when higher exposures on the CCD were used – at 1/100 dilutions, centers were bright indicating an uneven distribution of particles within the spots, likely due to too few particles per droplet. This effect decreased as the particle concentration increased. It was determined that the dilution range 1/60-1/80 would be appropriate for depositing particles with biotin functionality onto silicon surfaces, as these provided the highest density of functionality on the surface without introducing morphological abnormalities.

Covalent adhesion of PNIPAM-avidin particles deposition onto protein-reactive silicon surfaces was also evaluated. PNIPAM-avidin was diluted in either ddH_20 or mPBS (150 mM) to 1/60, 1/70, 1/80, 1/90, or 1/100 dilutions and the intensities of the central regions of each spot were analyzed and converted to thicknesses using AIR (Figure 4). After drying, spot morphologies were different between the two buffers; particles diluted in water had inconsistent morphologies at all dilutions, with bright centers and dark edges, and did not increase in thickness when the dilution decreased. Particles diluted in mPBS appeared highly uniform at all dilutions, and with thickness increases from 1/100 – 1/60, indicating that the packing was uniform and consistent. The difference between water and buffer was not surprising, as one would expect the high salt content of mPBS to screen electrostatic interactions between protein-laden nanoparticles during the drying process, as well as altering interactions with the surface.

To evaluate the assembly of particles in spots, particle packing characteristics were assessed by both scanning electron microscopy (SEM) and atomic force microscopy (AFM) (Figure 5).

Particles were found to be densely packed with uniform morphology as observed by SEM (Figure 5A). AFM confirmed that particles were packed in a dense monolayer (Figure 5B). Image analysis indicated that the particles were separated from the next closest (nearest neighbor) by an average distance of 500 ± 100 nm. A surface scan of a small region indicated that particles dried into flat disc-like shapes 300-400 nm wide and 3-7 nm tall (Figure 5C), similar to what has been observed by others.[45,52] Spot thicknesses and particle distributions within spots were thin and uniform and did not interfere with the performance of the AIR detection system. Protein-tagged particles strongly adhered to the substrates due

to the use of protein reactive surface chemistry. However, in our experience, particles also strongly adhered non-specifically, probably due to the strong electrostatic interactions between a flattened particle (high surface area) and the underlying substrate.

Target detection with hydrogel nanoparticle protein arrays using Arrayed Imaging Reflectometry (AIR)

Finally, hydrogel nanoparticle microspots were evaluated in the context of label-free detection. The cytokine, human tumor necrosis factor alpha (TNF-α), was chosen as a target. Aside from its importance in many biological processes, TNF-α is small (~17 kD) and is generally difficult to measure due to its low abundance in serum (1 – 10 pg/mL)[53,54] making it an ideal test case. Both biotinylated and non-biotinylated forms of anti-human TNF-α antibodies were used to selectively capture TNF-α. However, it was expected that only the biotinylated antibody would selectively conjugate onto PNIPAM-avidin.

PNIPAM-co-AA and PNIPAM-co-AA-biotin particles were printed onto protein reactive AIR substrates, blocked with 1% BSA block, and then incubated with 100 nM avidin, followed by 10 nM biotinylated TNF-α (b+a-TNF-α), and finally 10 nM human TNF-α (Figure 6). In addition to preventing non-specific adsorption of proteins, the blocking step was also important for maintaining spot morphology and consistency (Supplementary Figure S1).

The PNIPAM-co-AA spots were used as a control to monitor nonspecific binding of the different components. Results of the incubation showed specific binding of avidin, b+a-TNF-α IgG, and TNF-α to the PNIPAM-co-AA-biotin particles with total thickness increases of 0.51±0.04 nm, 1.15±0.06 nm, 1.66±0.05 nm respectively. Non-specific adsorption of the individual components to PNIPAM-co-AA were of 0.04±0.004 nm after avidin, 0.07±0.01 nm after IgG, and 0.2±0.03 after target. Neither of these thicknesses was as large as those seen for PNIPAM-co-AA-biotin. Minor amounts of nonspecific binding are likely due to the presence of 1% BSA as a carrier protein. The significant increase in thickness for the biotinylated particles indicated that the conjugation between hydrogel particle and biotinylated antibody was successful and could be used to detect targets.

Further experiments were conducted in which PNIPAM-avidin particles were pre-conjugated with biotinylated antibody and then printed, since this procedure would enable the creation of many particle-antibody pairs from the same starting particle.

PNIPAM-avidin particles were pre-mixed with non-biotinylated anti-human TNF-α IgG (a-TNF-α), biotinylated anti-human TNF-α (b+a-TNF IgG), and 1% BSA (as a control), and printed onto AIR substrates. The thicknesses of the resultant spots were measured by AIR (Figure 7). Results showed that particles selectively interacted with only biotinylated IgG molecules, as shown by the thickness difference (2.5±0.1 nm, versus −0.1±.0.2 nm). This thickness was also significantly different from the thickness added from only the 1% BSA carrier solution (0.1±0.1 nm). Furthermore, more total antibody was captured when pre-conjugating particles with antibodies rather than overspotting after first immobilizing PNIPAM-avidin.

Using this format, concentration dependent detection of TNF-α was examined. PNIPAM-avidin was pre-conjugated to +b-a-TNF-α IgG and printed with PNIPAM-co-AA-biotin (control) onto AIR substrates. Substrates were blocked with 1% BSA and exposed to different concentrations of TNF-α (1 pg/mL – 100 ng/mL, 10-fold steps). Spot thicknesses onto particle spots were determined by AIR, and the non-specific adsorption to PNIPAM-co-AA-biotin subtracted from the antibody coated particle spots. The results showed a thickness increase with increasing target concentration after subtracting the height of a substrate not exposed to target (Figure 8). The lowest concentration tested (1 pg/mL) was readily detectable; further optimization will be required to determine accurate limits of detection and quantitation for this assay format.

Conclusions

These combined data conclusively show that microspots of hydrogel nanoparticles can be successfully used to detect specific thickness increases with a highly sensitive label-free microarray technology. Currently available hydrogel polymerization techniques interfere with the sensing modalities of many label-free biosensors. As an alternative, we developed a hydrogel nanoparticle deposition method, which utilized the strong binding capability of avidin to generically couple probe molecules to particles. We demonstrated that these nanoparticles form uniform and reproducible monolayers that are less than 10 nm thin, which can be arrayed simply and easily on surfaces. Using a highly sensitive label-free biosensor, we showed the potential of this method to detect targets.

The data we have acquired to date suggest that the hydrogel arrays provide sensitivity similar to, if not better than, AIR assays in which antibodies are directly coupled to the surface.[42] While optimization should improve this further, we anticipate that this methodology will yield advantages beyond analytical sensitivity, including: enhanced shelf life due to the hydrogel matrix, and more rapid development time as starting spot thicknesses depend primarily on the hydrogel rather than on the reactivity of the protein (which can vary considerably from antibody to antibody). Efforts to test these hypotheses are in progress, along with development of a particle/probe conjugate library to detect multiple targets on a single substrate. While tested here in the context of antibody deposition, we expect this methodology will prove equally useful for the preparation of nucleic acid-based or small molecule arrays. Likewise, this strategy should work equally well for other sensor platforms.

Supplementary Material

Refer to Web version on PubMed Central for supplementary material.

ACKNOWLEDGMENT

This work was supported by the National Institutes of Health (NIGMS grant R01GM100788). M.A.L. was supported by the Training Grant in HIV Biology, NIH-NIAID T32AI049815-12.

REFERENCES

(1). Parpia ZA, Kelso DM. Anal. Biochem. 2010; 401:1–6. [PubMed: 20152793]

(2). Ekins RP. Clin. Chem. 1998; 44:2015–2030. [PubMed: 9733000]
(3). Ekins RP, Chu FW. Clin. Chem. 1991; 37:1955–1967. [PubMed: 1934470]
(4). MacBeath G, Schreiber SL. Science (80−.). 2000; 289:1760–1763.
(5). MacBeath G. Nat. Genet. 2002; 32:526–532. [PubMed: 12454649]
(6). Robinson WH, et al. Nat. Med. 2002; 8:295–301. [PubMed: 11875502]
(7). Stoll D, Templin MF, Schrenk M, Traub PC, Vohringer CF, Joos TO. Front. Biosci. 2002; 7:C13–C32. [PubMed: 11779717]
(8). Falsey JR, Renil M, Park S, Li S, Lam KS. Bioconjug. Chem. 2001; 12:346–353. [PubMed: 11353531]
(9). Houseman BT, Huh JH, Kron SJ, Mrksich M. Nat. Biotechnol. 2002; 20:270–274. [PubMed: 11875428]
(10). Shumaker-Parry JS, Aebersold R, Campbell CT. Anal. Chem. 2004; 76:2071–2082. [PubMed: 15053673]
(11). Halpern AR, Chen Y, Corn RM, Kim D. Anal. Chem. 2011; 83:2801–2806. [PubMed: 21355546]
(12). Cretich M, Monroe MR, Reddington A, Zhang X, Daaboul GG, Damin F, Sola L, Unlu MS, Chiari M. Proteomics. 2012; 12:2963–2977. [PubMed: 22930463]
(13). Yu C, Lopez C. a. Hu H, Xia Y, Freedman DS, Reddington AP, Daaboul GG, Ünlü MS, Genco CA. PLoS One. 2014; 9
(14). Dufva M. Biomol. Eng. 2005; 22:173–184. [PubMed: 16242381]
(15). Brown CS, Goodwin PC, Sorger PK. Proc. Natl. Acad. Sci. U. S. A. 2001; 98:8944–8949. [PubMed: 11481466]
(16). Xu H, Lu JR, Williams DE. J. Phys. Chem. B. 2006; 110:1907–1914. [PubMed: 16471762]
(17). Kosaka PM, Tamayo J, Ruz JJ, Puertas S, Polo E, Grazu V, de la Fuente JM, Calleja M. Analyst. 2013; 138:863–872. [PubMed: 23223515]
(18). Chen S, Liu L, Zhou J, Jiang S. Langmuir. 2003; 19:2859–2864.
(19). Butler JE, Ni L, Nessler R, Joshi KS, Suter M, Rosenberg B, Chang J, Brown WR, Cantarero LA. J. Immunol. Methods. 1992; 150:77–90. [PubMed: 1613260]
(20). O'Brien JC, Jones VW, Porter MD, Mosher CL, Henderson E. Anal. Chem. 2000; 72:703–710. [PubMed: 10701253]
(21). Ibii T, Kaieda M, Hatakeyama S, Shiotsuka H, Watanabe H, Umetsu M, Kumagai I, Imamura T. Anal. Chem. 2010; 82:4229–4235. [PubMed: 20415430]
(22). Buenger D, Topuz F, Groll J. Prog. Polym. Sci. 2012; 37:1678–1719.
(23). Byun J-Y, Lee K-H, Lee K-Y, Kim M-G, Kim D-M. Lab Chip. 2013; 13:886–891. [PubMed: 23303405]
(24). Angenendt P. Progress in protein and antibody microarray technology. Drug Discovery Today. 2005; 10:503–511. [PubMed: 15809196]
(25). Sugaya S, Kakegawa S, Fukushima S, Yamada M, Seki M. Langmuir. 2012; 28:14073–14080. [PubMed: 22991929]
(26). Massad-Ivanir N, Shtenberg G, Zeidman T, Segal E. Adv. Funct. Mater. 2010; 20:2269–2277.
(27). Wilkins Stevens P, Wang CHJ, Kelso DM. Anal. Chem. 2003; 75:1141–1146. [PubMed: 12641234]
(28). Zubtsov DA, Savvateeva EN, Rubina AY, Pan'kov SV, Konovalova EV, Moiseeva OV, Chechetkin VR, Zasedatelev AS. Anal. Biochem. 2007; 368:205–213. [PubMed: 17544357]
(29). Rubina AY, Dementieva EI, Stomakhin AA, Darii EL, Pan'kov SV, Barsky VE, Ivanov SM, Konovalova EV, Mirzabekov AD. Biotechniques. 2003; 34:1008–1022. [PubMed: 12765028]
(30). Rubina AY, Dyukova VI, Dementieva EI, Stomakhin AA, Nesmeyanov VA, Grishin EV, Zasedatelev AS. Anal. Biochem. 2005; 340:317–329. [PubMed: 15840505]
(31). Olle EW, Messamore J, Deogracias MP, McClintock SD, Anderson TD, Johnson KJ. Exp. Mol. Pathol. 2005; 79:206–209. [PubMed: 16246325]
(32). Charles PT, Goldman ER, Rangasammy JG, Schauer CL, Chen MS, Taitt CR. Biosens. Bioelectron. 2004; 20:753–764. [PubMed: 15522590]

(33). Derwinska K, Sauer U, Preininger C. Anal. Biochem. 2007; 370:38–46. [PubMed: 17679102]
(34). Feuz L, JÖnsson P, Jonsson MP, HÖÖk F. ACS Nano. 2010; 4:2167–2177. [PubMed: 20377272]
(35). Pal S, Yadav AR, Lifson MA, Baker JE, Fauchet PM, Miller BL. Biosens. Bioelectron. 2013; 44:229–234. [PubMed: 23434758]
(36). Ishikawa E, Hashida S, Kohno T. Mol. Cell. Probes. 1991; 5:81–95. [PubMed: 2072938]
(37). Waggoner PS, Craighead HG. Lab Chip. 2007; 7:1238–1255. [PubMed: 17896006]
(38). Vollmer F, Braun D, Libchaber a. Khoshsima M, Teraoka I, Arnold S. Appl. Phys. Lett. 2002; 80:4057–4059.
(39). Lu J, Strohsahl CM, Miller BL, Rothberg LJ. Anal. Chem. 2004; 76:4416–4420. [PubMed: 15283581]
(40). Horner SR, Mace CR, Rothberg LJ, Miller BL. Biosens. Bioelectron. 2006; 21:1659–1663. [PubMed: 16154335]
(41). Mace CR, Striemer CC, Miller BL. Biosens. Bioelectron. 2008; 24:334–337. [PubMed: 18599284]
(42). Carter JA, Mehta SD, Mungillo MV, Striemer CC, Miller BL. Biosens. Bioelectron. 2011; 26:3944–3948. [PubMed: 21474297]
(43). Mace CR, Topham DJ, Mosmann TR, Quataert S. a. Treanor JJ, Miller BL. Talanta. 2011; 83:1000–1005. [PubMed: 21147350]
(44). Yadav AR, Mace CR, Miller BL. Anal. Chem. 2014; 86:1067–1075. [PubMed: 24377303]
(45). Tsuji S, Kawaguchi H. Langmuir. 2005; 21:8439–8442. [PubMed: 16114954]
(46). Pelton R. Adv. Colloid Interface Sci. 2000; 85:1–33. [PubMed: 10696447]
(47). Zhou XC, Huang LQ, Li SFY. Biosens. Bioelectron. 2001; 16:85–95. [PubMed: 11261857]
(48). Huang G, Gao J, Hu Z, St. John JV, Ponder BC, Moro D. J. Control. Release. 2004; 94:303–311. [PubMed: 14744482]
(49). Sriram R, Yadav AR, MacE CR, Miller BL. Anal. Chem. 2011; 83:3750–3757. [PubMed: 21517019]
(50). Lee KS, Drescher DG. Int. J. Biochem. 1978; 9:457–467. [PubMed: 28966]
(51). NanoComposix. Nanocomposix's Guide to Dynamic Light Scattering Measurement and Analysis. San Diego: 2012.
(52). Tsuji S, Kawaguchi H. E-Polymers. 2005; 21:1–7.
(53). Anderson NL, Anderson NG. Mol. Cell. Proteomics. 2002; 1:845–867. [PubMed: 12488461]
(54). Arican O, Aral M, Sasmaz S, Ciragil P. Mediators Inflamm. 2005; 2005:273–279. [PubMed: 16258194]

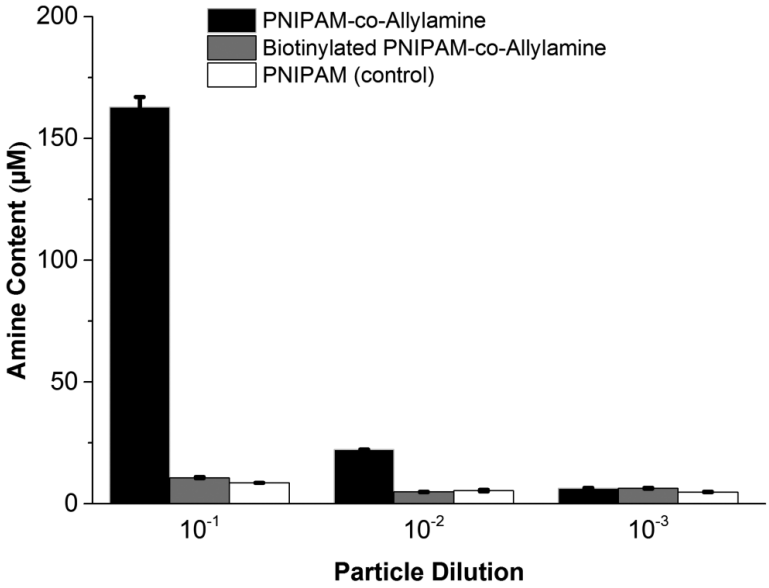

Figure 1.

Quantification of amines present in 4 different dilutions of PNIPAM (white bar), PNIPAM-co-Allylamine (black solid bar), and PNIPAM-co-Allylamine conjugated to biotin (gray bar) using an o-phthaldealdehyde assay. Fluorescence measurements (n=3) were performed at 460 nm (emission, 360 nm excitation) and averaged. Error bars represent standard deviations from these measurements.

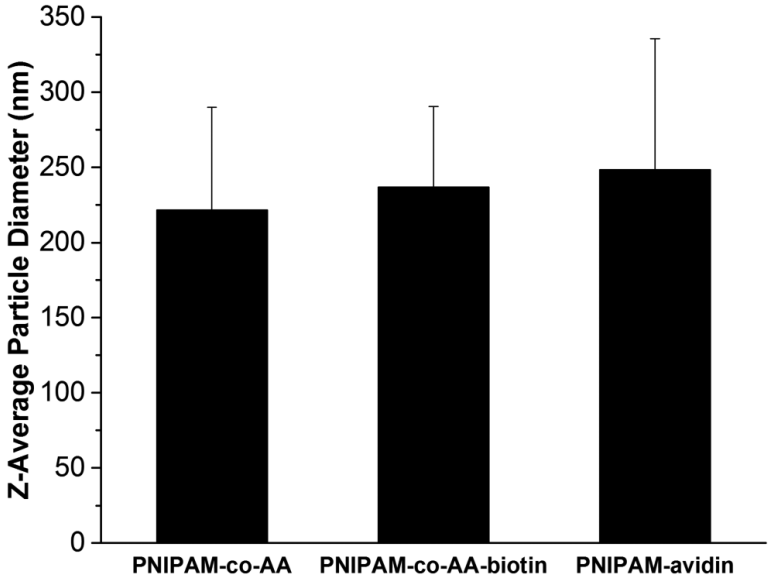

Figure 2.

Dynamic light scattering evaluation of PNIPAM-co-AA Z-average particle diameters through different stages of conjugation. The original particle (left bar) was covalently biotinylated using an NHS-biotin linker (middle bar). Avidin was then bound to the particle-conjugated biotin. Error bars represent standard deviations calculated from the square-root of the polydispersity index multiplied by the z-average diameter. The conjugation procedure had no significant effect on particle diameter.

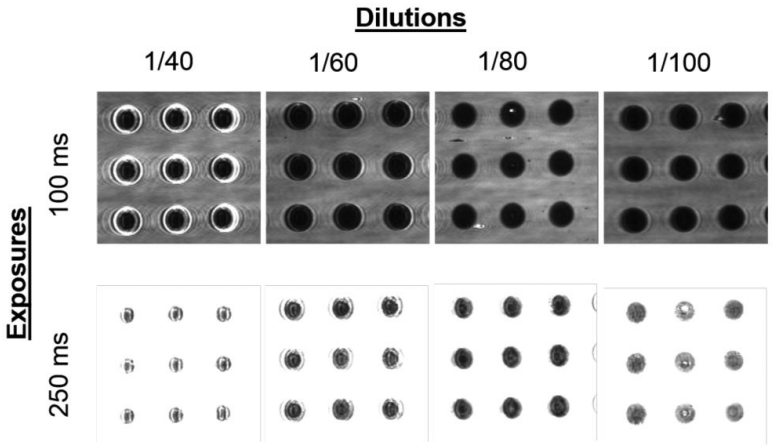

Figure 3.

AIR images of PNIPAM-co-AA at two different exposures (100 ms and 250 ms) printed on silicon substrates at 1/40, 1/60, 1/80, and 1/100 dilutions.

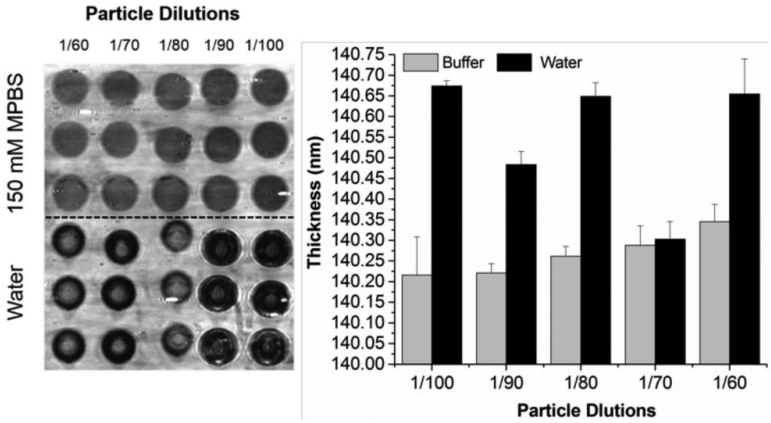

Figure 4.

Dried AIR image (left) and average thickness measurements (right) of PNIPAM-avidin diluted in either ddH2O or mPBS buffer at 1/60, 1/70, 1/80, 1/90, or 1/100 concentrations and printed onto protein reactive silicon substrates. Error bars represent standard deviations of average values (n = 3).

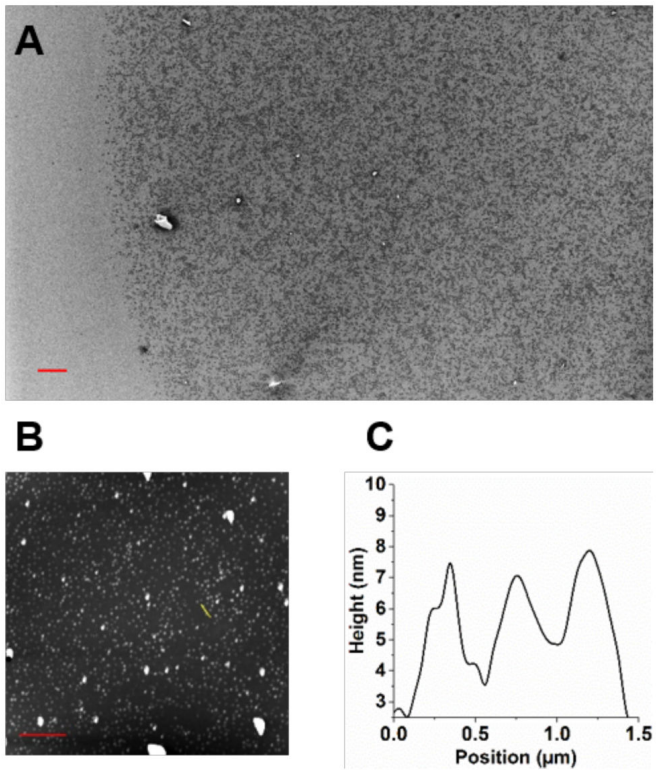

Figure 5.

Morphological analysis of dry, self-assembled PNIPAM-avidin particles after deposition with a piezoelectric microarrayer (~300 pL volume droplet). SEM image showing a droplet edge (A) indicated densely packed particles in a monolayer. AFM analysis of the surface (B) corroborated the packing behavior of the dried particle droplets observed with SEM, and a profile of a small portion of the surface (highlighted in yellow) indicated that the particles flattened to ~500 nm widths and ~4 nm heights (C). Scale bars (red lines in A, B) are 5 μm.

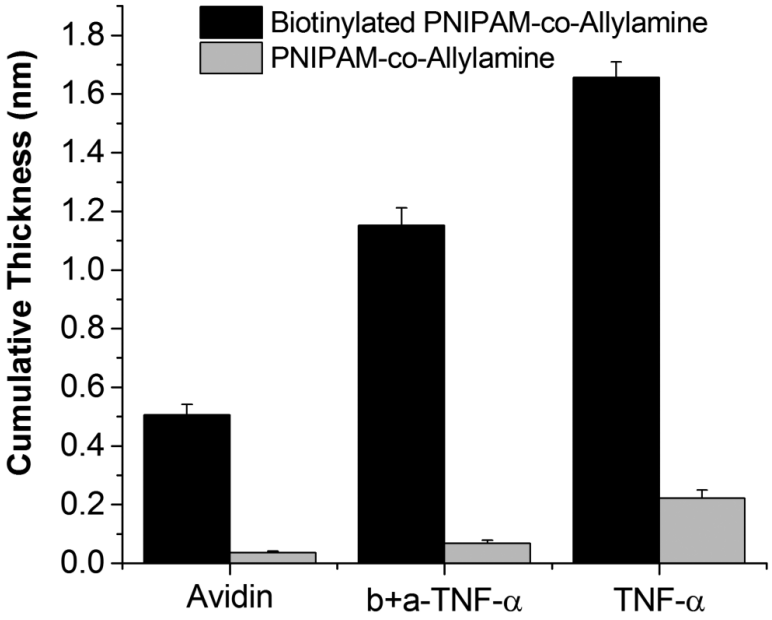

Figure 6.

Average spot thickness as measured with AIR on immobilized PNIPAM-co-AA (gray bar) and PNIPAM-co-AA-biotin (black bar) after consecutive staged incubation with avidin, followed by 10 nM biotinylated anti-human TNF-α (b+TNF-α), and ending with 10 nM TNF-α target detection (TNF-α). Error bars are reported as standard deviations from averaged measurements (n>3).

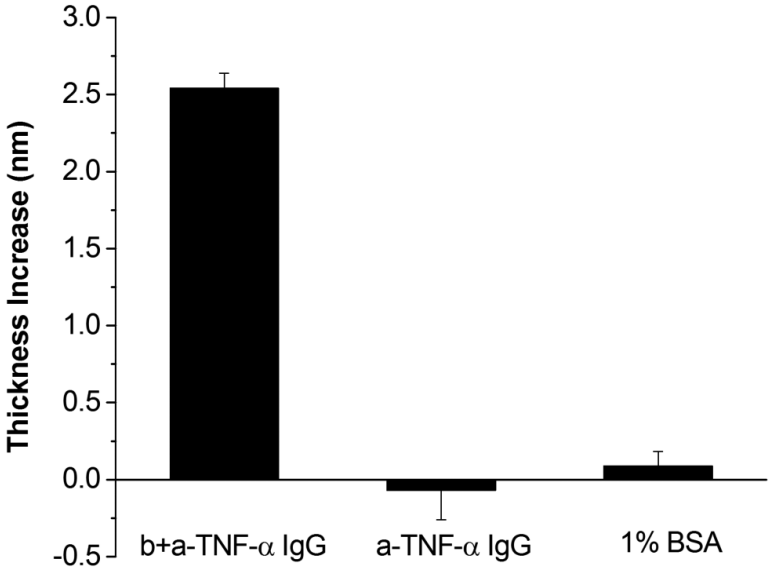

Figure 7.

AIR average measurements (n=35) of avidinylated PNIPAM-co-A nanoparticle spots after incubation with either biotinylated anti-human TNF-α IgG (b+a-TNF-α), anti-human TNF-α IgG (a-TNF-α), or 1% BSA in PBS, showing thickness changes relative to PNIPAM-avidin particles alone. Error bars are standard deviations of average measurements.

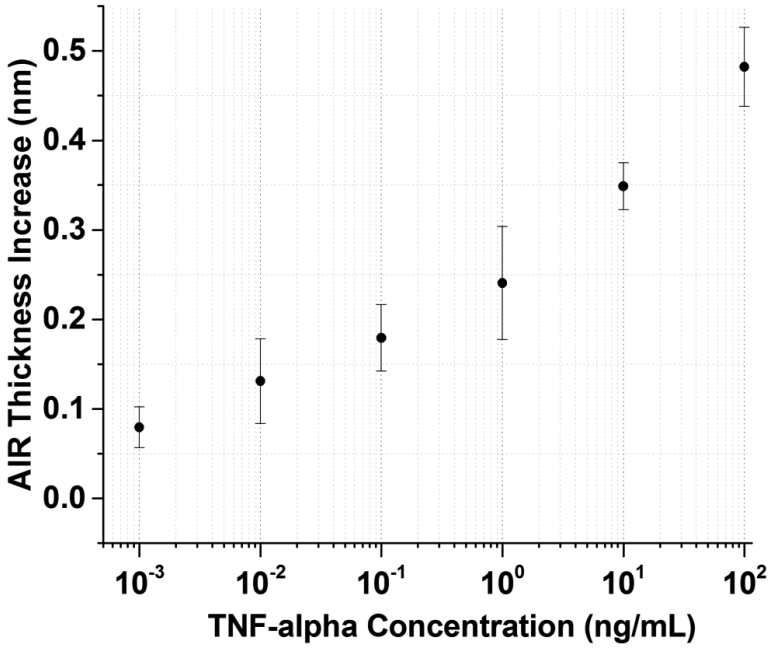

Figure 8.

AIR spot thickness measurements (n>3) of immobilized PNIPAM-co-AA pre-conjugated with anti-human TNF-α IgG spots, incubated with different concentrations of TNF-α target. Thickness increases were calculated by subtracting the measured height of an equivalent substrate that was not exposed to target. Results show an increasing dose-response with concentration of target. Error bars are standard deviations of average measurements.